**A Thesis**

**For the Degree of Master of Science in Medicine**

# Photo-protective effect of sargachromenol against UVB radiation-induced damage through modulating cellular antioxidant systems and apoptosis in human keratinocytes

Graduate School, Jeju National University

Department of Medicine

**Pattage Madushan Dilhara Jayatissa Fernando**

August, 2016

**A Thesis**

**For the Degree of Master of Science in Medicine**

# Photo-protective effect of sargachromenol against UVB radiation-induced damage through modulating cellular antioxidant systems and apoptosis in human keratinocytes

Graduate School, Jeju National University

Department of Medicine

**Pattage Madushan Dilhara Jayatissa Fernando**

August, 2016

# 인간각질형성세포에서 자외선 B로 유도되는 항산화 시스템의 조절과 세포사멸을 통한 세포손상에 대한 sargachromenol의 광보호 작용

지도교수 현 진 원

**마두샨 페르난도**

이 논문을 석사학위 논문으로 제출함

2016년 8월

마두샨 페르난도의 석사학위 논문을 인준함

심사위원장 박 덕 배 印

위 원 강 희 경 印

위 원 현 진 원 印

제주대학교대학원

2016년 8월

# Photo-protective effect of sargachromenol against UVB radiation-induced damage through modulating cellular antioxidant systems and apoptosis in human keratinocytes

**Pattage Madushan Dilhara Jayatissa Fernando**

(Supervised by professor Jin Won Hyun)

A thesis submitted for the partial fulfilment of the requirement for the degree of Master of Science in Medicine

August, 2016

This thesis has been examined and approved.

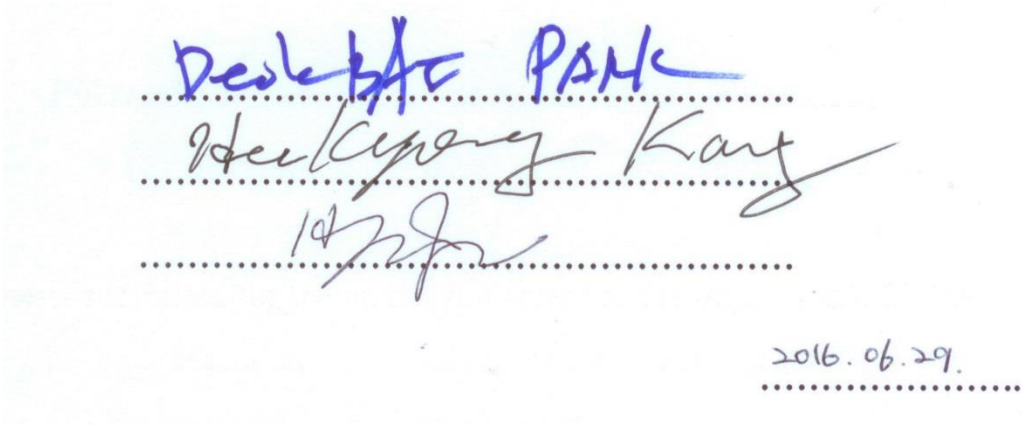

Department of Medicine

GRADUATE SCHOOL

JEJU NATIONAL UNIVERSITY

## Abstract

The aim of this study was to evaluate the photochemopreventive effects of sargachromenol (SC) against ultraviolet B (UVB)-induced oxidative stress in human keratinocytes via assessing the antioxidant properties and underlying molecular mechanisms. SC exhibited a significant scavenging effect on UVB-induced intracellular reactive oxygen species (ROS). SC attenuated UVB-induced oxidative macromolecular damage, including the protein carbonyl content, DNA strand breaks, and 8-isoprostane level. Furthermore, SC decreased UVB-induced Bax, cleaved caspase-9, and cleaved caspase-3 protein levels, but increased that of Bcl-2, which are well-known key mediators of apoptosis. Moreover, SC increased superoxide dismutase, catalase, and heme oxygenase-1 protein expression. Pre-treatment with SC upregulated the total nuclear factor erythroid 2-related factor 2 (Nrf2) levels, which was reduced by UVB irradiation, indicating the involvement of the Nrf2-antioxidant response element signaling pathway. Jun N-terminal kinases (JNK) and extracellular signal-regulated kinase (ERK) are involved in the regulation of many cellular events, including apoptosis. SC treatment reversed JNK and ERK activation induced by UVB. Collectively, these data indicate that SC can provide remarkable cytoprotection against the adverse effects of UVB radiation by modulating cellular antioxidant systems, and suggest the potential of developing a medical agent for ROS-induced skin diseases.



*Keyword:* Sargachromenol, reactive oxygen species, ultraviolet B radiation, human keratinocytes

# Content

## List of Figures

# 1. **Introduction**

Skin, the largest human organ, is the protective covering of the body and is daily exposed to environmental stress sources. Skin is naturally exposed to excessive levels of ultraviolet (UV) radiation, resulting in the generation of debilitating levels of intracellular reactive oxygen species (ROS) (Lee et al., 2014). Ultraviolet B (UVB) irradiation-induced ROS upregulate the inflammatory response in the skin through the impairment of its natural antioxidant system (Martinez et al., 2015).

UVB radiation (280–320 nm) stimulates ROS generation and oxidative stress in the skin (Hewage et al., 2015). Chronic UVB exposure induces inflammation including erythema, premature aging, edema formation, immunosuppression, and skin cancer. UVB accelerates photo-oxidative reactions that can alter anti-ROS-sensitive signaling pathways, which ultimately increases the cellular ROS level (Yogianti et al., 2012). Moreover, toxic products basically derived via protein carbonylation and lipid peroxidation cause extensive oxidative damage. UVB irradiation especially damages keratinocytes of the epidermis through the generation of DNA damage in the form of cyclobutane pyrimidine dimers (CPDs), which has been implicated in the risk of skin cancer (Choi et al., 2014). Interleukin-6 and tumor necrosis factor-α are inflammatory cytokines that were previously reported to be associated with UVB exposure (Heck et al., 2004). Accumulated studies emphasize that mitogen-activated protein kinases (MAPKs) are essential for UVB-induced apoptosis of human keratinocytes and UV-induced cellular responses such as skin cancer.

Skin has the ability to counteract UVB-induced ROS via efficient antioxidant defense mechanisms. When ROS generation overwhelms this antioxidant defense capacity, the ability of the skin to recover from damage caused by ROS is impaired, leading to oxidative damage of

cellular macromolecules such as DNA, proteins, and lipids (Saw et al., 2014).

Nowadays, natural compounds are focused upon as a means to improve human health due to their low toxicity and safety. Meanwhile, the supplementation of dietary botanical antioxidants against UVB-induced oxidative injuries has been frequently studied. Sargachromenol (SC, Fig. 1A), a compound isolated from the brown marine alga *Sargassum micracanthum*, has various pharmacological properties, including antioxidant and antiviral activities (Yang et al., 2013). SC has also neuroactive properties via promoting neurite outgrowth and supporting the survival of neuronal PC12D cells (Hur et al., 2008).

## 2. **Materials and Methods**

### 2-1. Reagents

SC isolated from *Sargassum macrocarpum* was kindly donated by Professor Nam Ho Lee of Jeju National University (Jeju, Republic of Korea). Diphenyl-2-picrylhydrazyl (DPPH), 2',7'-dichlorodihydrofluorescein diacetate (DCF-DA), 3-(4,5-dimethylthiazol-2-yl)-2,5-diphenyltetrazolium bromide (MTT), Hoechst 33342, N-acetyl cysteine (NAC), 5,5-dimethyl-1-pyrroline-N-oxide (DMPO), and anti-actin antibody were purchased from Sigma-Aldrich Corporation (St. Louis, MO, USA). Diphenyl-1-pyrenylphosphine (DPPP) was purchased from Molecular Probes (Eugene, OR, USA). An anti-superoxide dismutase (Cu/Zn SOD) antibody was purchased from Enzo Life Sciences (Farmingdale, NY, USA). Antibodies against catalase (CAT), heme oxygenase-1 (HO-1), Nrf2, extracellular signal-regulated kinase (ERK)-2, phospho ERK, Bax, Bcl-2 and caspase-9 were purchased from Santa Cruz Biotechnology (Dallas, TX, USA). Anti-caspase-3, Phospho JNK and JNK antibodies were purchased from Cell Signaling Technology (Danvers, MA, USA). All other chemicals and reagents were of analytical grade.

### 2-2. Cell culture and UVB irradiation

Human keratinocytes (HaCaT cells) obtained from Amore Pacific Company (Yongin, Republic of Korea) were maintained at 37℃ in an incubator with a humidified atmosphere of 5% $CO_2$. The cells were cultured in RPMI 1640 medium containing 10% heat-inactivated fetal calf serum, streptomycin (100 μg/mL), and penicillin (100 U/mL). The UVB source was a CL-1000M UV Crosslinker (UVP, Upland, CA, USA), which was used to deliver an energy spectrum of UVB radiation (280–320 nm; peak intensity, 302 nm). Cells were exposed to 30 $mJ/cm^2$ UVB

**2-3. Cell viability**

Cells were treated with SC (2.5, 5, 10, 20, or 40 μM) and exposed to UVB radiation 1 h later. They were then incubated at 37℃ for 48 h. At this time, MTT was added to each well to obtain a total reaction volume of 200 μL. After incubation for 4 h, the supernatant was removed by aspiration. The formazan crystals in each well were dissolved in dimethyl sulfoxide (DMSO; 150 μL), and the absorbance at 540 nm was measured on a scanning multi-well spectrophotometer (Carmichael et al., 1987).

**2-4. DPPH radical detection**

SC (2.5, 5, 10, 20, or 40 μM) or 1 mM NAC was added to 0.1 mM DPPH and incubated for 30 min. Subsequently, the amount of residual DPPH was determined by measuring absorbance at 520 nm using a spectrophotometer.

**2-5. Intracellular ROS detection**

Intracellular ROS levels in the human keratinocytes were measured by the DCF-DA assay (Rosenkranz et al., 1992). Cells were seeded at a density of $1.5 \times 10^5$ cells/well in 24-well culture plates. Sixteen hours after plating, cells were treated with SC (2.5, 5, 10, 20, or 40 μM) or 1 mM NAC. After incubation for 30 min, cells were exposed to $H_2O_2$ (1 mM) and again incubated for 30 min. $H_2O_2$-treated cells were treated with DCF-DA (25 μM) and incubated for another 10 min to detect the fluorescence of DCF. Otherwise, cells were incubated with SC (40 μM) or 1 mM NAC for 1 h and exposed to UVB (30 mJ/cm$^2$). After 24 h, cells were further incubated with DCF-DA for 10 min. The fluorescence of DCF was detected using a PerkinElmer LS-5B spectrofluorometer (PerkinElmer, Waltham, MA, USA). In order to analyze intracellular ROS by fluorescence microscope, cells were seeded on a four-well chamber slide at $1\times10^5$

cells/mL density. Sixteen hours later, cells were treated with 40 μM SC, incubated for 1 hour, and irradiated with UVB light. After an additional 20 h, 40 μM of DCF-DA was added to each well, and the samples were incubated for further 30 min at 37℃. After washing with PBS, stained cells were mounted on the chamber slide in mounting medium. Images were captured by the confocal microscope using the LSM 5 PASCAL software (Carl Zeiss, Jena, Germany).

**2-6. Detection of the superoxide anion**

The superoxide anion was produced via the xanthine/xanthine oxidase system and reacted with a nitrone spin trap, DMPO. The DMPO/·OOH adducts were detected using a JES-FA electron spin resonance (ESR) spectrometer (JEOL, Tokyo, Japan) (Kohno et al., 1994). Briefly, ESR signaling was recorded 5 min after 20 μL of xanthine oxidase (0.25 unit/mL) was mixed with 20 μL each of xanthine (5 mM), DMPO (1.5 M), and SC (40 μM). The ESR spectrometer parameters were set as follows: magnetic field, 336 mT; power, 1.00 mW; frequency, 9.438 GHz; modulation amplitude, 0.2 mT; gain, 500; scan time, 0.5 min; scan width, 10 mT; time constant, 0.03 sec; and temperature, 25℃.

**2-7. Detection of the hydroxyl radical**

The hydroxyl radical was generated via the Fenton reaction ($H_2O_2$ + $FeSO_4$) and reacted with DMPO. The resultant DMPO/·OH adducts were detected using an ESR spectrometer (Li et al., 2004). The ESR spectrum was recorded 2.5 min after a phosphate buffer solution (pH 7.4) was mixed with 0.2 mL each of DMPO (0.3 M), $FeSO_4$ (10 mM), $H_2O_2$ (10 mM), and SC (40 μM). The ESR spectrometer parameters were as follows: magnetic field, 336 mT; power, 1.00 mW; frequency, 9.438 GHz; modulation amplitude, 0.2 mT; gain, 200; scan time, 0.5 min; scan width, 10 mT; time constant, 0.03 sec; and temperature, 25℃.

**2-8. UV/visible light absorption analysis**

The ability of SC to absorb UV radiation was investigated by scanning this compound with UV/visible light in the 200-400 nm range. Absorption values for specific wavelengths by SC (40 μM) diluted in dimethyl sulfoxide (DMSO) was measured by using a Biochrom Libra S22 UV/visible spectrophotometer (Biochrom Ltd., Cambridge, UK).

**2-9. Lipid peroxidation assay**

Lipid peroxidation was assayed by colorimetric determination of the levels of 8-isoprostane, a stable end product of lipid peroxidation, in medium from HaCaT cells (Beauchamp et al., 2002). Level of 8-isoprostane was measured using a commercial enzyme immune assay (Cayman Chemical, Ann Arbor, MI, USA). Lipid peroxidation was additionally assessed using DPPP as a probe. DPPP reacts with lipid hydroperoxides to generate a fluorescent product, DPPP oxide, thereby providing an indication of membrane damage. Cells were treated with 40 μM SC for 1 h and exposed to UVB (30 $mJ/cm^2$) for 24 h. After that, cells were incubated with 20 μM DPPP for 30 min in the dark. Images of DPPP fluorescence were captured on a Zeiss Axiovert 200 inverted microscope at an excitation wavelength of 351 nm and an emission wavelength of 380 nm.

**2-10. Protein carbonyl formation**

Cells were treated with SC at a concentration of 40 μM for 24 h. One hour later, cells were exposed to UVB and incubated at 37℃ for another 24 h. The level of protein carbonyl formation was measured using an Oxiselect™ protein carbonyl ELISA kit from Cell Biolabs (San Diego, CA, USA).

**2-11. Single-cell gel electrophoresis (comet assay)**

The Comet assay was performed to assess the oxidative DNA damages in individual cells (Singh, 2000). Cells were treated with SC (40 μM), 1 h later, exposed to UVB light (30 mJ/cm$^2$), centrifuged at 13,000 × g for 5 min to collect the cell suspension. The cell suspension was mixed with 70 μL of 1% low-melting agarose (LMA) at 37℃, and the mixture was spread onto a fully frosted microscope slide pre-coated with 200 μL of 1% normal-melting agarose. Agarose was allowed to solidify, slides were covered with another 170 μL of 0.5% LMA and immersed in lysis solution (2.5 M NaCl, 100 mM Na-EDTA, 10 mM Tris, 1% Triton X-100, and 10% DMSO, pH 10) for 1 h at 4℃. These slides were then electrophoresed in a gel electrophoresis apparatus containing 300 mM NaOH and 10 mM Na-EDTA (pH 10) and allowed to unwind the DNA under alkaline/neutral conditions by incubating for 30 min. An electrical field (300 mA, 25 V) was then applied for 30 min at 25℃ to draw the negatively-charged DNA towards the anode. The slides were dipped in neutralizing buffer (0.4 M Tris, pH 7.5) three times for 10 min at 25℃, and again washed once for 10 min at 25℃ in 100% ethanol. Slides were stained with 80 μL of 10 μg/mL ethidium bromide, a DNA-specific fluorescent dye and observed using a fluorescence microscope and image analyzer (Kinetic Imaging, Komet 5.5, UK). Tail length and percentage of total fluorescence in the comet tails were recorded for 50 cells per slide.

**2-12. Nuclear staining with Hoechst 33342**

Cells were treated with 40 μM SC and exposed to 30 mJ/cm$^2$ UVB radiation 1 h later. After incubation for an additional 24 h at 37℃, 1 μL of the DNA-specific fluorescent dye Hoechst 33342 (stock, 15 mM) was added to each well of the 6-well plate. The plate was then incubated for 10 min at 37℃. The degree of nuclear condensation in the stained cells was determined by

visualization with a fluorescence microscope equipped with a CoolSNAP-Pro color digital camera.

### 2-13. Western blot analysis

Cells were harvested and lysed by incubation in 150 μL of lysis buffer (iNtRON Biotechnology, Republic of Korea) on ice. The cells lysates were collected and centrifuged at 13,000 × *g* for 5 min. Resultant Supernatants were analyzed for protein concentration. Aliquots (each containing 5 μg of protein) were boiled for 5 min and electrophoresed on 12% SDS-polyacrylamide gels. After the separation of the proteins, transfer of proteins to the nitrocellulose membrane was done. Appropriate primary antibodies against target proteins were used to incubate membranes. Membranes were further incubated with secondary immunoglobulin G-horseradish peroxidase conjugates. Proteins bands were then detected by developing the blots using an enhanced chemiluminescence Western blotting detection kit (Amersham, Buckinghamshire, UK) and exposing the membranes to X-ray film.

### 2-14. Statistical analysis

All measurements were performed in triplicate, and all values are expressed as means ± standard error. The results were subjected to an analysis of variance using Tukey's test to analyze differences between means. In all cases, $p < 0.05$ was considered to be statistically significant.

# 3. Results

## 3-1. Effect of SC on UVB-induced ROS generation

At the experimental concentrations of 2.5, 5, 10, 20, and 40 μM SC didn't show any significant cytotoxicity on HaCaT keratinocytes (Fig. 1B). SC scavenged the DPPH radical in a concentration-dependent manner, with 16%, 21%, 25%, 33%, and 51% of radicals scavenged when the concentration of SC was 2.5, 5, 10, 20, and 40 μM, respectively. These results were compared with that obtained with the positive control, NAC (1 mM) (Fig. 1C). $H_2O_2$-induced intracellular ROS-scavenging activity was measured at different concentrations of SC. This activity was 29% with 40 μM SC, whereas the corresponding activity for NAC was 38% (Fig. 1D). Considering these results, 40 μM SC was chosen as the optimal dose for further experiments. Next, the scavenging effects of SC on the superoxide anion and hydroxyl radical were measured by ESR spectrometry. The superoxide anion signal from the xanthine/ xanthine oxidase system yielded a value of 2819 compared to 668 in the control, while SC reduced this value to 2052 (Fig. 1E). Similarly, the hydroxyl radical signal in the Fenton reaction ($Fe^{2+} + H_2O_2 \rightarrow Fe^{3+} + \cdot OH + OH^-$) was increased to a value of 3846 in comparison to 70 in the control; however, SC reduced this value to 2198 (Fig. 1F). The intracellular ROS-generation against SC was next measured in UVB-treated cells. SC and NAC treatment significantly reduced the ROS generation in UVB-treated human keratinocytes (Fig. 1G). In addition, fluorescence microscopy analysis of ROS was performed. The green fluorescence intensity, which correlated with the ROS level, demonstrated that SC could decrease the level of ROS generated upon UVB irradiation (Fig. 1H). As demonstrated by UV/visible light spectrophotometry (Fig. 1I), SC had a significant absorptive capacity (peak, 225 nm). Therefore, the light-absorbing property of SC

may be closely related to the cytoprotection against UVB irradiation.

**A**

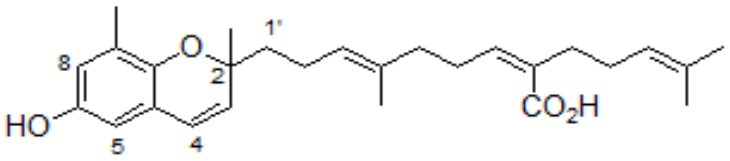


**B**

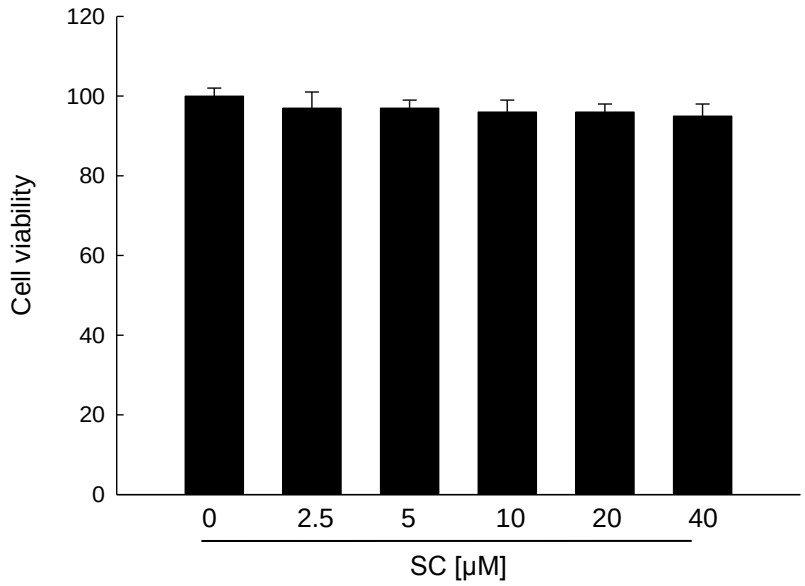


z

**C**

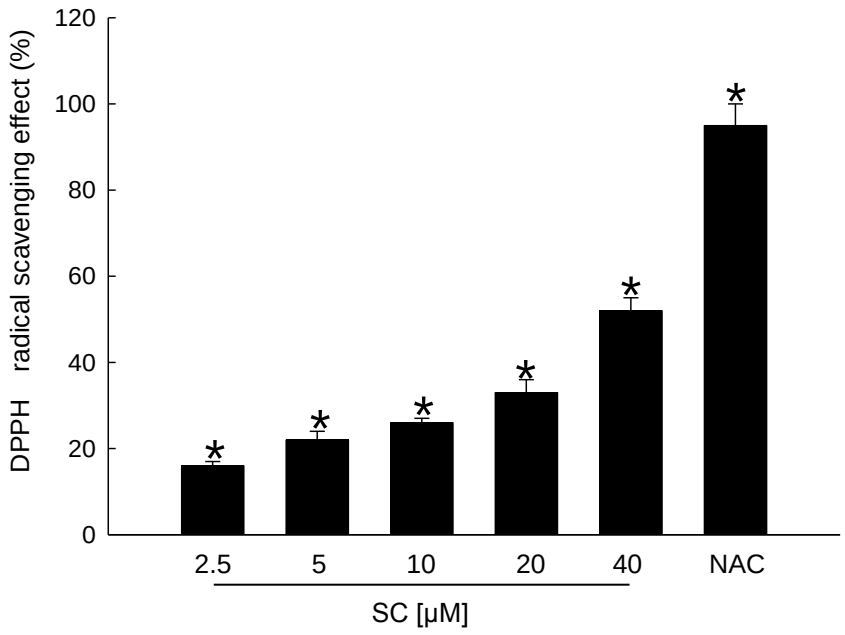

**D**

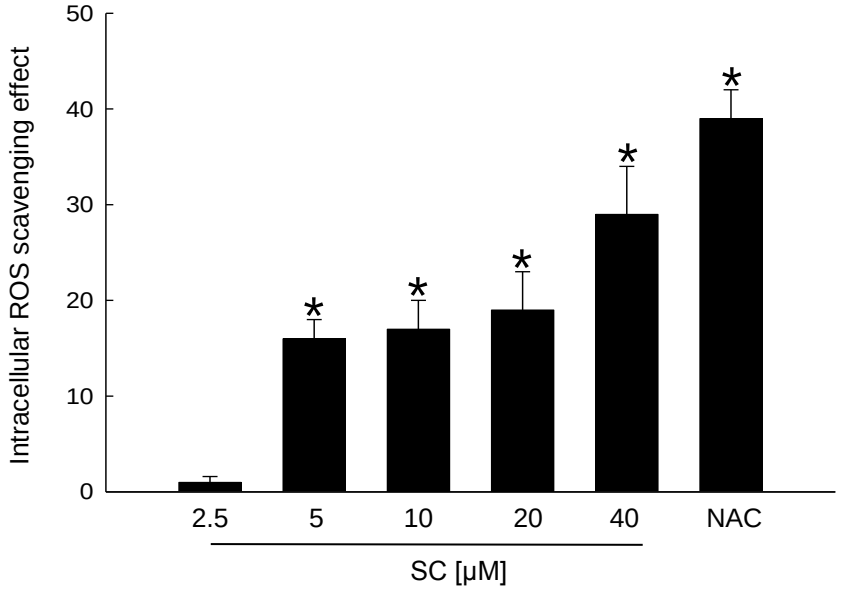


**E**

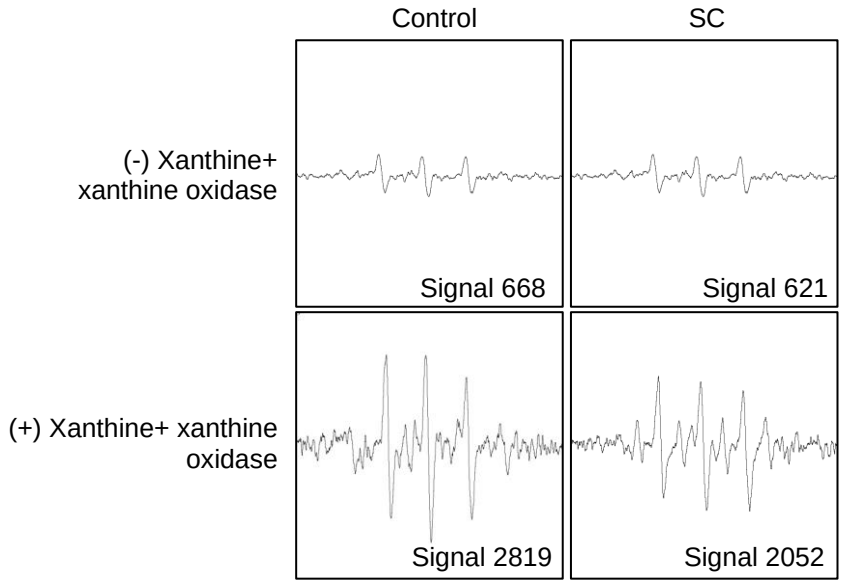


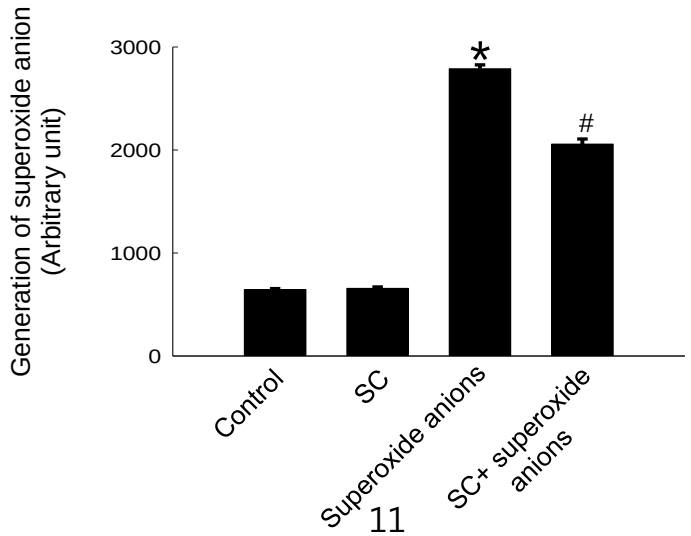

**F**

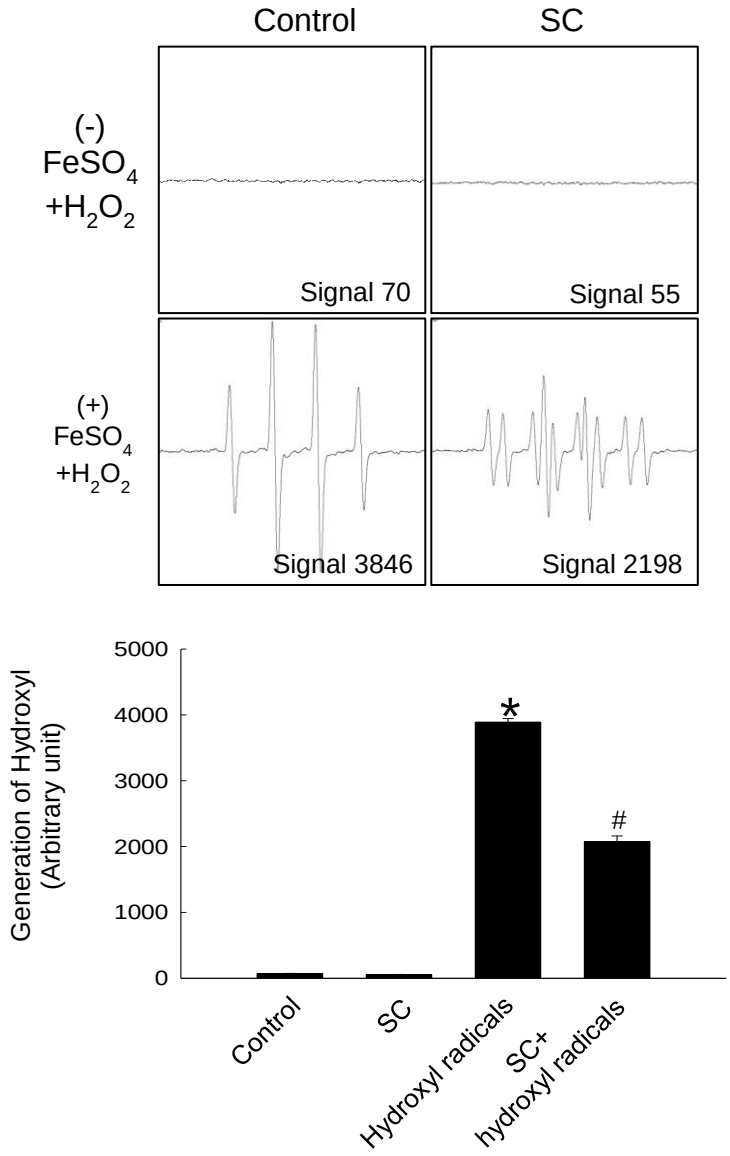


**G**

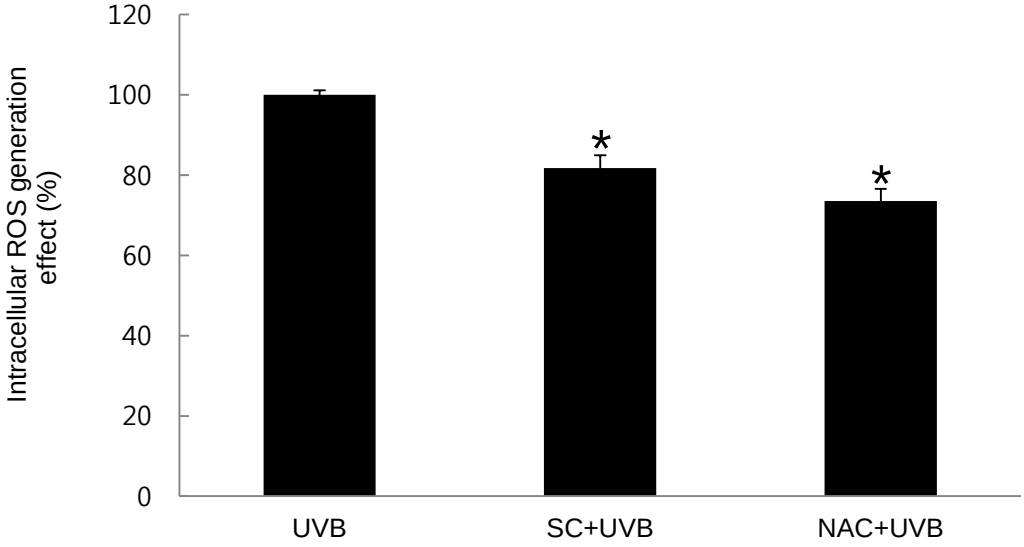

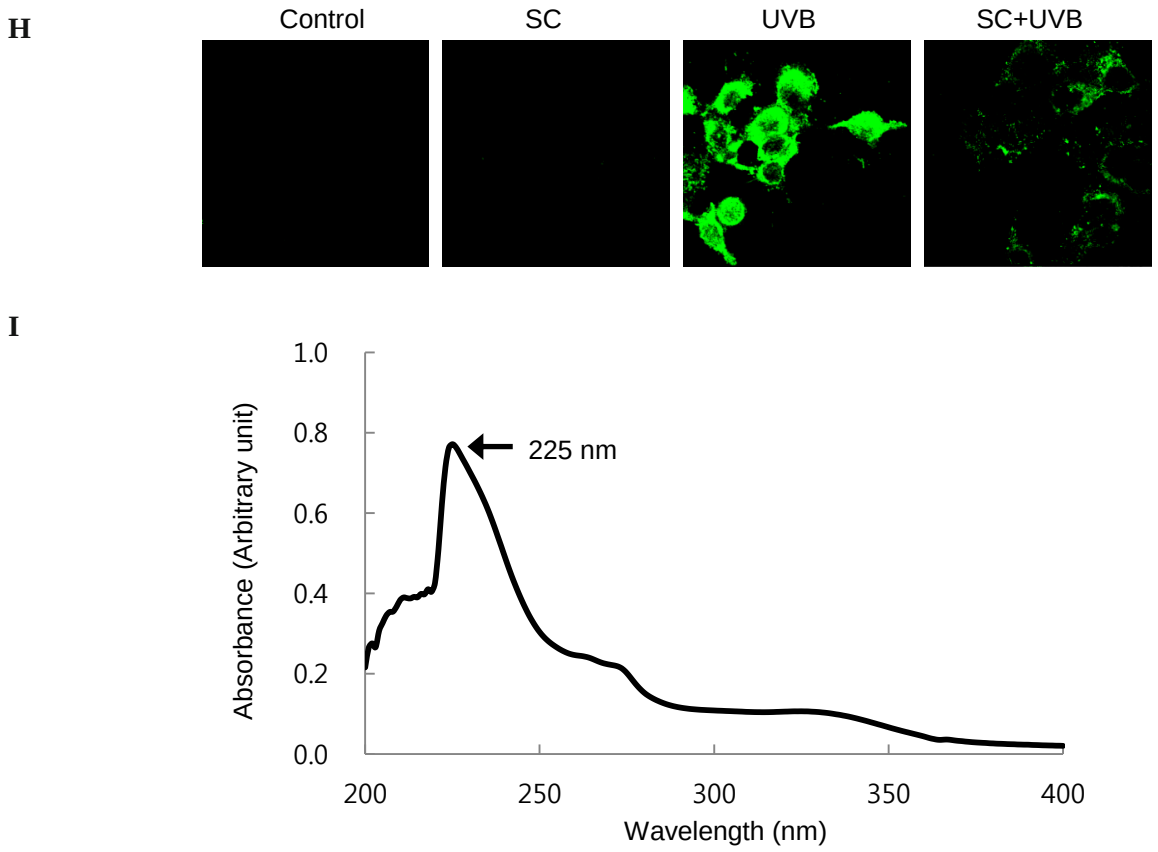


**Figure. 1. Scavenging of free radicals by SC**. (A) Chemical structure of sargachromenol ($C_{27}H_{36}O_4$). (B) HaCaT cells were treated with SC (2.5, 5, 10, 20, or 40 μM) for 20 h. Cell viability was measured in the MTT assay. (C) Scavenging of the DPPH radical was measured spectrophotometrically at 520 nm. NAC (1 mM) served as the positive control. *Significantly different from control cells ($p < 0.05$). (D) The scavenging of intracellular ROS generated by $H_2O_2$ was measured by the DCF-DA assay. *Significantly different from control cells ($p < 0.05$). (E), (F) The ability of SC to scavenge superoxide and hydroxyl radicals was evaluated using the Fenton reaction ($FeSO_4 + H_2O_2$ system) and the xanthine/xanthine oxidase system, respectively, and quantified. (G) Scavenging of intracellular ROS generated by UVB was evaluated in the DCF-DA assay. *Significantly different from control cells ($p < 0.05$). (H) Representative confocal microscopy images illustrate the increase in the green fluorescence intensity in UVB-

exposed cells compared with control cells. (I) The UVB absorption spectrum of SC was analyzed at 200–400 nm. The arrow represents the absorbance peak at 225 nm.

### 3-2. SC attenuates UVB-induced macromolecular damage in HaCaT cells

Intracellular ROS induced by UVB radiation in the skin provoke damage to cellular macromolecules such as proteins, mitochondrial and nuclear DNA, and lipids (Aoki et al., 2014). We investigated the potential of SC to attenuate membrane lipid peroxidation, cellular DNA damage, and protein carbonylation in UVB-irradiated cells. The level of 8-isoprostane was notably increased in UVB-irradiated cells, while SC treatment significantly inhibited this elevation (Fig. 2A). Lipid peroxidation was additionally monitored using DPPP. DPPP, which stoichiometrically reacts with lipid hydroperoxides to yield the highly fluorescent product DPPP oxide, was used as a fluorescent probe to assess lipid peroxidation in live cells. The blue fluorescence intensity of DPPP oxide was increased in UVB-irradiated cells, but this was remarkably reduced in SC-treated cells (Fig. 2B). Formation of protein carbonyl groups is a reliable biomarker of oxidative stress due to their early formation and relative stability (Dalle-Donne et al., 2003). The protein carbonyl level was increased in UVB-irradiated cells, whereas SC treatment significantly suppressed UVB-induced carbonyl formation (Fig. 2C). Cellular DNA damage influenced by UVB was measured by the comet assay. This assay is used to detect DNA damage by measuring DNA damage in individual cells and estimating its distribution in cell populations. UVB irradiation of HaCaT cells increased the percentage of DNA in the tails by 56% in comparison with the control group, and SC treatment was able to recover this value to 35% (Fig. 2D).

**A**

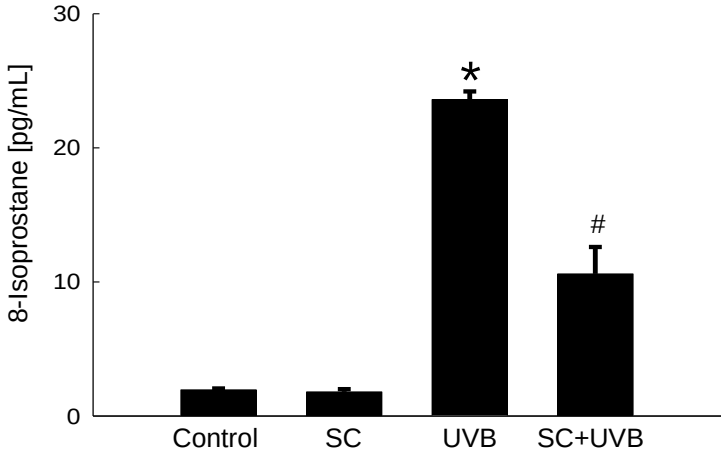


**B**

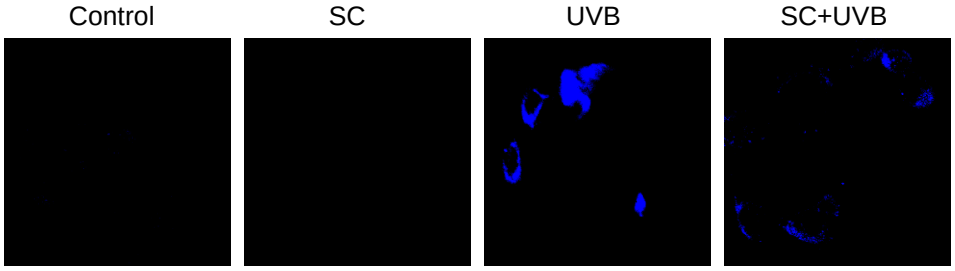


**C**

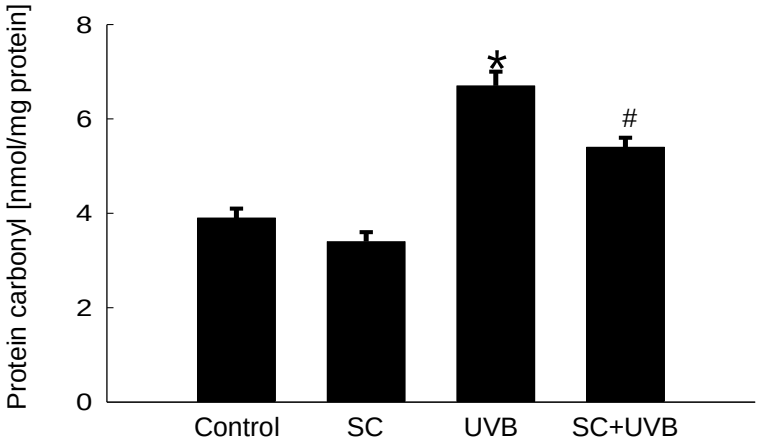


**D**

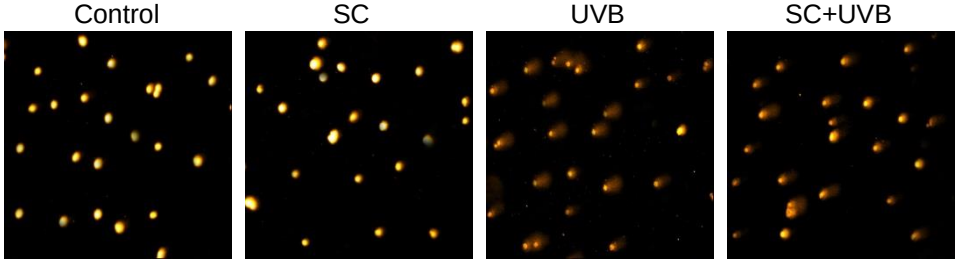

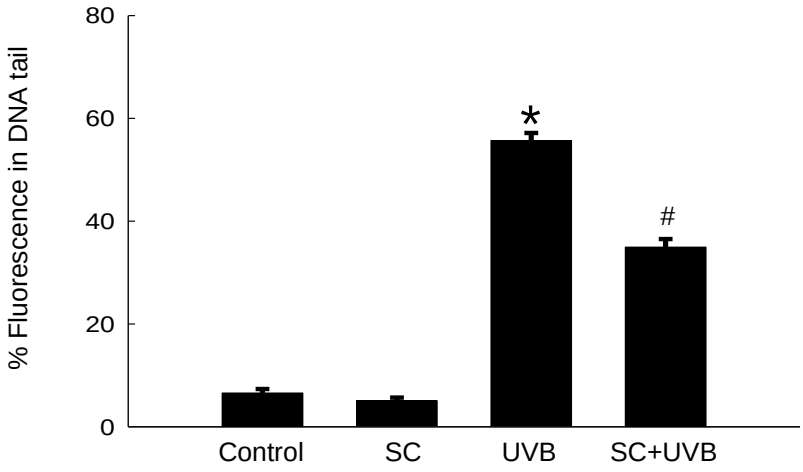


**Figure. 2. SC protects HaCaT cells against UVB-induced oxidative lipid damage, protein, DNA, and. Cells were treated with 40 μM SC for 1 h, and then exposed to UVB**. (A) Lipid peroxidation was assessed by measuring 8-isoprostane levels in conditioned medium. *Significantly different from control cells ($p < 0.05$); #significantly different from UVB-irradiated cells ($p < 0.05$). (B) Representative confocal microscopy images illustrate the increase in the blue fluorescence intensity of DPPP oxide produced by lipid hydroperoxides in UVB-exposed cells compared with control cells. (C) Protein oxidation was assayed by the level of protein carbonyls, a marker of protein oxidation. *Significantly different from control cells ($p < 0.05$); #significantly different from UVB-irradiated cells ($p < 0.05$). (D) The comet assay was used to assess DNA damage. Representative images and percentages of cellular fluorescence within comet tails are shown. *Significantly different from control cells ($p < 0.05$); #significantly different from UVB-irradiated cells ($p < 0.05$).

### 3-3. Effect of SC against apoptosis induced by UVB radiation

Accumulated data show that UVB-induce apoptosis in human keatinocytes (Lee and Park, 2014). Therefore, we next investigated whether SC affects the viability of UVB-irradiated cells. The MTT assay demonstrated that cell viability was improved from 55% (UVB-irradiated cells)

to 74% when cells were pre-treated with SC prior to UVB irradiation (Fig. 3A). The cytoprotective effect of SC against UVB-induced apoptosis was further studied by staining nuclei with Hoechst 33342 and performing microscopy.

Intact nuclei were observed in control cells, whereas significant numbers of apoptotic bodies, which are characterized by nuclear fragmentation, were found in UVB-exposed cells. Interestingly, the formation of apoptotic bodies was dramatically reduced in UVB-exposed keratinocytes pre-treated with SC. These results were similar to those obtained in cells pre-treated with 1 mM NAC (Fig. 3B). To study the effect of SC on UVB-induced cell death, we evaluated the expression levels of Bax, Bcl-2, caspase-9, and caspase-3 proteins in keratinocytes pre-treated with SC and then irradiated with UVB. In UVB-irradiated cells, pro-apoptotic Bax, caspase-9, and caspase-3 were activated, while expression of anti-apoptotic Bcl-2 was decreased. However, SC treatment markedly decreased the protein expression levels of Bax, cleaved caspase-9, and cleaved caspase-3 in UVB-irradiated cells. Furthermore, the Bcl-2 level was clearly reduced in UVB-irradiated keratinocytes (Fig. 3C).

**A**

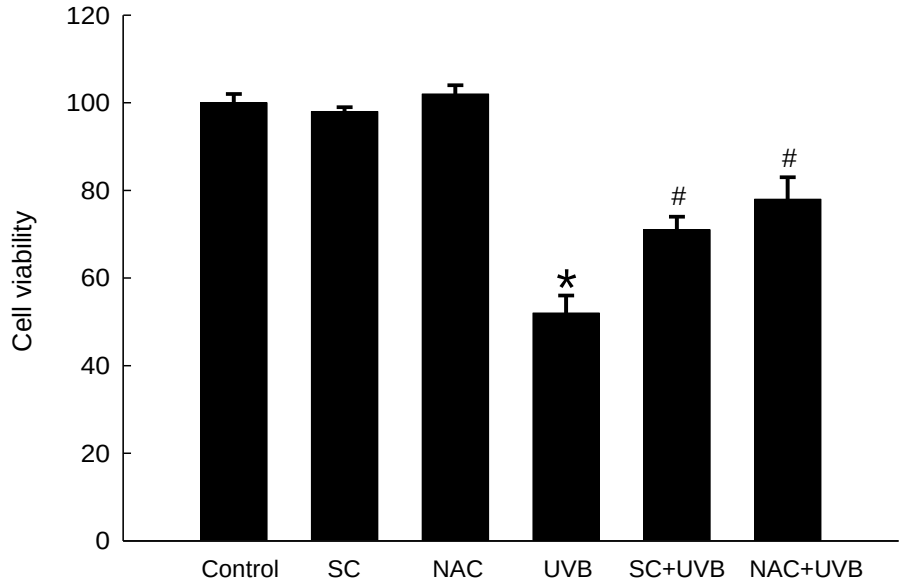

**B**

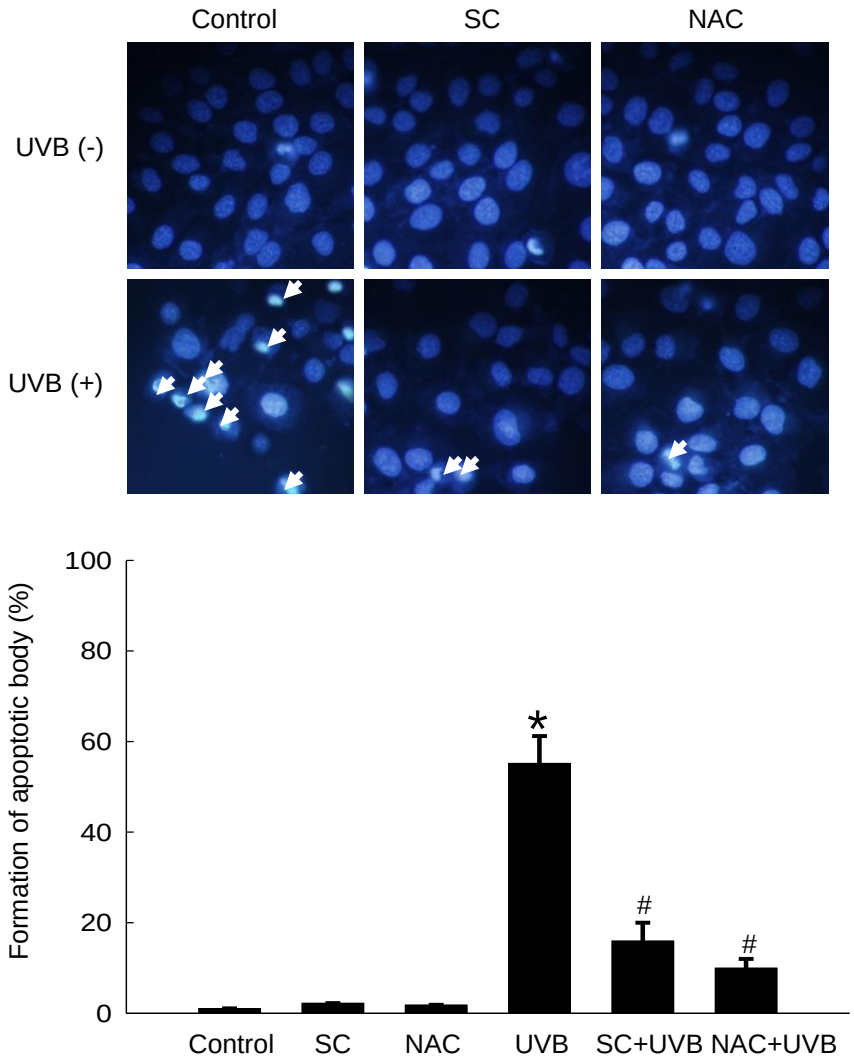


**D**

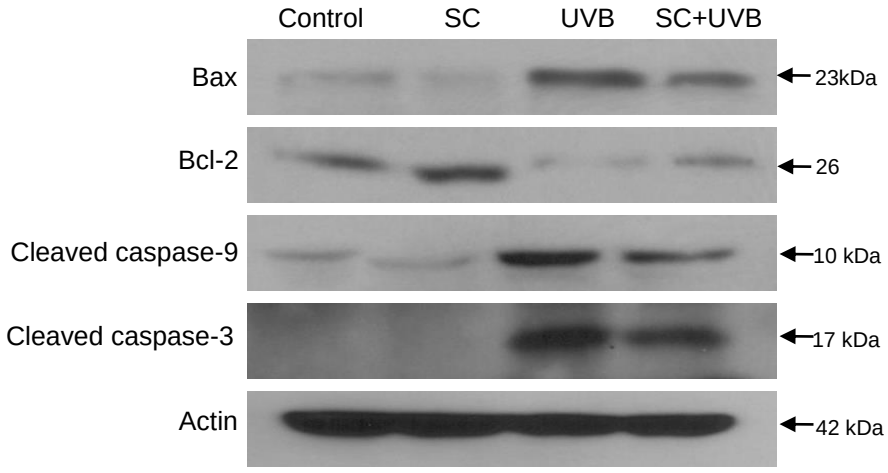

**Figure. 3. SC protects cells from UVB-induced apoptosis.** (A) Cells were pre-treated with 40 μM SC or 1 mM NAC, and then exposed to UVB (30 mJ/cm$^2$). Cell viability was measured in the MTT assay. *Significantly different from control cells ($p < 0.05$); $^{\#}$significantly different from UVB-irradiated cells ($p < 0.05$). (B) Cells were stained with Hoechst 33342 dye, and apoptotic bodies (arrows) were observed by fluorescence microscopy and quantitated. (C) Cell lysates were subjected to electrophoresis. Bax (23 kDa), Bcl-2 (26 kDa), cleaved caspase-9 (10 kDa), and caspase-3 (17 kDa) were immunoblotted using appropriate antibodies. Actin was used as a loading control.

### 3-4. Effect of SC on the protein expression levels of antioxidant enzymes and the Nrf2-antioxidant response element pathway

To elucidate the effect of SC on skin-derived antioxidant enzymes, the protein expression levels of Cu/Zn SOD, CAT, and HO-1 in SC-treated cells were determined. Protein expression of Cu/Zn SOD, CAT, and HO-1 was markedly reduced in UVB-irradiated cells; however, pre-treatment with SC enhanced these protein levels in UVB-irradiated cells (Fig. 4A). Many phytochemicals exert their antioxidant activity via activation of the Nrf2-antioxidant response element pathway; therefore, we investigated the involvement of Nrf2 in SC-mediated cytoprotection. The level of Nrf2 was markedly reduced in keratinocytes irradiated with UVB; however, pre-treatment with SC increased the level of Nrf2 compared with that in UVB-irradiated cells (Fig. 4B).

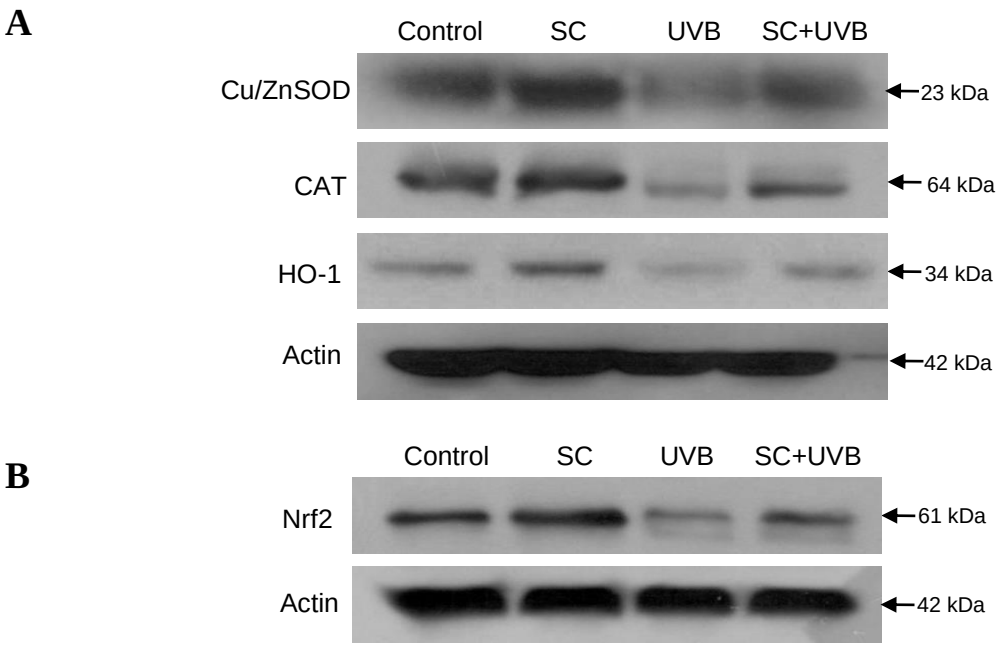


**Figure. 4. SC enhances antioxidant systems that are perturbed by UVB irradiation. HaCaT cells were treated with 40 μM SC for 1 h, and then exposed to UVB**. (A) Cell lysates were subjected to gel electrophoresis, and then Western blot analysis was performed using antibodies against Cu/Zn SOD, CAT, and HO-1. Actin was used as a loading control. (B) Protein expression level of Nrf2 (total).

### 3-5. Effects of SC on ERK and JNK signal transduction

JNK and ERK, stress-activated MAPKs, are involved in many cellular regulatory processes, including apoptosis. Therefore, the protein expression levels of ERK and JNK were analyzed to elucidate the mechanism by which SC protects against UVB-induced oxidative damage. As shown in results, UVB-irradiated cells had elevated levels of activated JNK and ERK. Therefore, our findings demonstrate that SC can suppress UVB-induced phospho-JNK and phospho-ERK levels and thus be used to prevent UVB-

induced cell damage (Fig. 5).

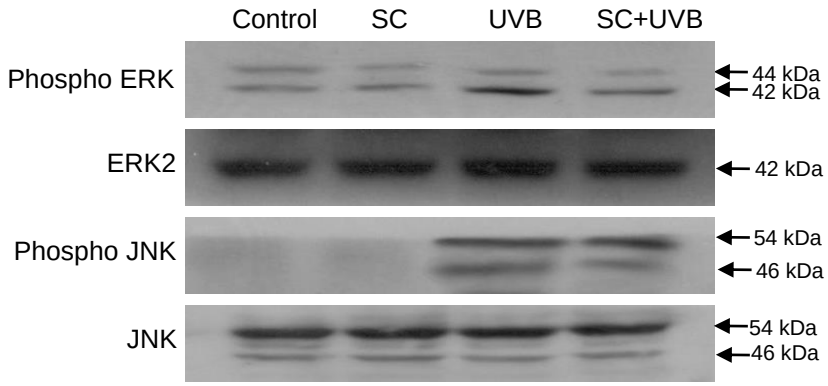


**Figure. 5.** Effects of SC on ERK and JNK signal transduction. Cell lysates were electrophoresed and phospho-ERK and phospho-JNK were detected using specific antibodies.

## 4. Discussion

UVB radiation emitted from the sun penetrates the dermis of the skin and is epidemiologically proven to be a main cause of skin cancers. Recently, various plant-derived phytochemicals have been extensively investigated because they possess anti-inflammatory and antioxidant properties, and thus exert photoprotective effects on the skin (Kim et al., 2014). *S. micracanthum* is a widespread marine alga from which a number of biologically important substances are isolated. Among these, SC is one of the main components and is experimentally proven to have various pharmacological properties including antiviral, antioxidant, and anti-inflammatory effects (Yang et al., 2013). SC has been previously studied in terms of its neuronal growth factor function and anti-cholinesterase activity (Kim et al., 2014). To our knowledge, no previous study has revealed antioxidant-mediated cytoprotection by SC or the signaling pathways that underlie its ability to protect against UVB-induced oxidative damage in human keratinocytes.

UVB irradiation primarily initiates molecular responses via the generation of ROS. Antioxidants are of a natural origin and therefore hold great promise as an effective strategy to eliminate the occurrence of UVB-induced oxidative damage and skin cancer. In the current study, SC treatment significantly reduced the level of ROS induced by UVB irradiation, proving its antioxidant potential. When ROS accumulate in biological systems without being scavenged, they can encourage many biochemical alterations such as inflammation, DNA damage, oxidation of lipids and proteins, and dysfunction of certain enzymes.

Cellular membrane lipids are highly vulnerable to peroxidation, which leads to impaired cellular function, loss of elasticity, and even cell rupture (Ambothi and Nagarajan, 2014). Here, we discovered that SC prevents lipid peroxidation induced by UVB irradiation in human

keratinocytes. Carbonyl groups (aldehydes and ketones) are formed on the side chains of proteins as a result of their oxidation. Prolonged accumulation of protein carbonyls may either alter cellular regulatory pathways or disrupt cellular functions. Our results clearly indicated that SC also reduced protein carbonyl formation provoked by UVB irradiation. Furthermore, DNA tails in the comet assay indicated that SC could prevent oxidative DNA strand breaks induced by UVB irradiation.

UVB basically targets DNA and induces DNA damage, especially CPDs and (6-4) photoproducts, ultimately causing mutations in skin cells and leading to the progression of cancer and apoptosis (Ichihashi et al., 2003). The molecular mechanisms underlying UVB-induced apoptosis include DNA strand damage (intrinsic pathway), clustering of death receptors on the cell surface (extrinsic pathway), and ROS generation. According to our results, UVB-exposed cells were characterized by the formation of apoptotic bodies, reduced cell viability, induction of pro-apoptotic protein expression, and reduction of anti-apoptotic protein expression. Notably, SC protected keratinocytes from UVB-induced apoptosis.

Overproducing free radicals can be scavenged by endogenous antioxidant enzymes to protect cellular components from ROS-induced damages in mammalian cells. A range of antioxidant enzymes are reported to mediated in this process including ROS scavengers such as, HO-1, CAT, Cu/Zn SOD as well as glutathione peroxidase (GPx). HO-1 is the rate-limiting enzyme in the catabolism of the pro-oxidant heme and functions antioxidant protein. Cu/Zn SOD is basically involved in the conversion of superoxide ($O_2^-$) to hydrogen peroxide ($H_2O_2$) and these $H_2O_2$ is reduced $H_2O$ via the activity of CAT. In the present study we found that SC could markedly elevate the UVB suppressed antioxidant protein expression in human keratinocytes, which most likely indicates a cytoprotective response to oxidative stress.

Nrf2 is the master regulator of the antioxidant response which regulates the expression of various antioxidant enzymes. In the present report, UVB exposure led to the suppression of Nrf2 and attenuation of antioxidant enzymes, while SC treatment could recover this significantly. Considering the current data, we assume that cellular exposure to the SC induces Nrf2 translocation into the nucleus and enhance the transcription of antioxidant enzymes. Meanwhile exact mechanism lied behind SC-induced Nrf2 up regulation is to be elucidated in future studies.

The ERK signaling pathway is activated by UVB-induced ROS in human keratinocytes (Dhanasekaran and Reddy, 2008). JNK, a stress-activated MAPK, reportedly regulates many cellular processes, including apoptosis (Widel et al., 2014). SC could strongly block ERK and JNK activation induced by UVB irradiation, suggesting that activation of ERK and JNK MAPKs is involved in the cytoprotective role of SC.

Collectively, in the present study, we elucidated the cytoprotective role of SC against UVB irradiation (Fig. 6); SC effectively attenuated UVB-induced apoptosis and macromolecular damage, including DNA damage, protein carbonylation, lipid peroxidation, and antioxidant depletion, by scavenging UVB-induced ROS. In addition, our study demonstrated that the protective effect of SC was mediated by the Nrf2-antioxidant response element pathway. Our findings suggest that ERK and JNK MAPKs are involved in this process; however, the underlying mechanisms remain to be explored. Therefore, intervention with SC could be a promising approach to prevent photo-damage and to develop a therapeutic photo-protective agent.

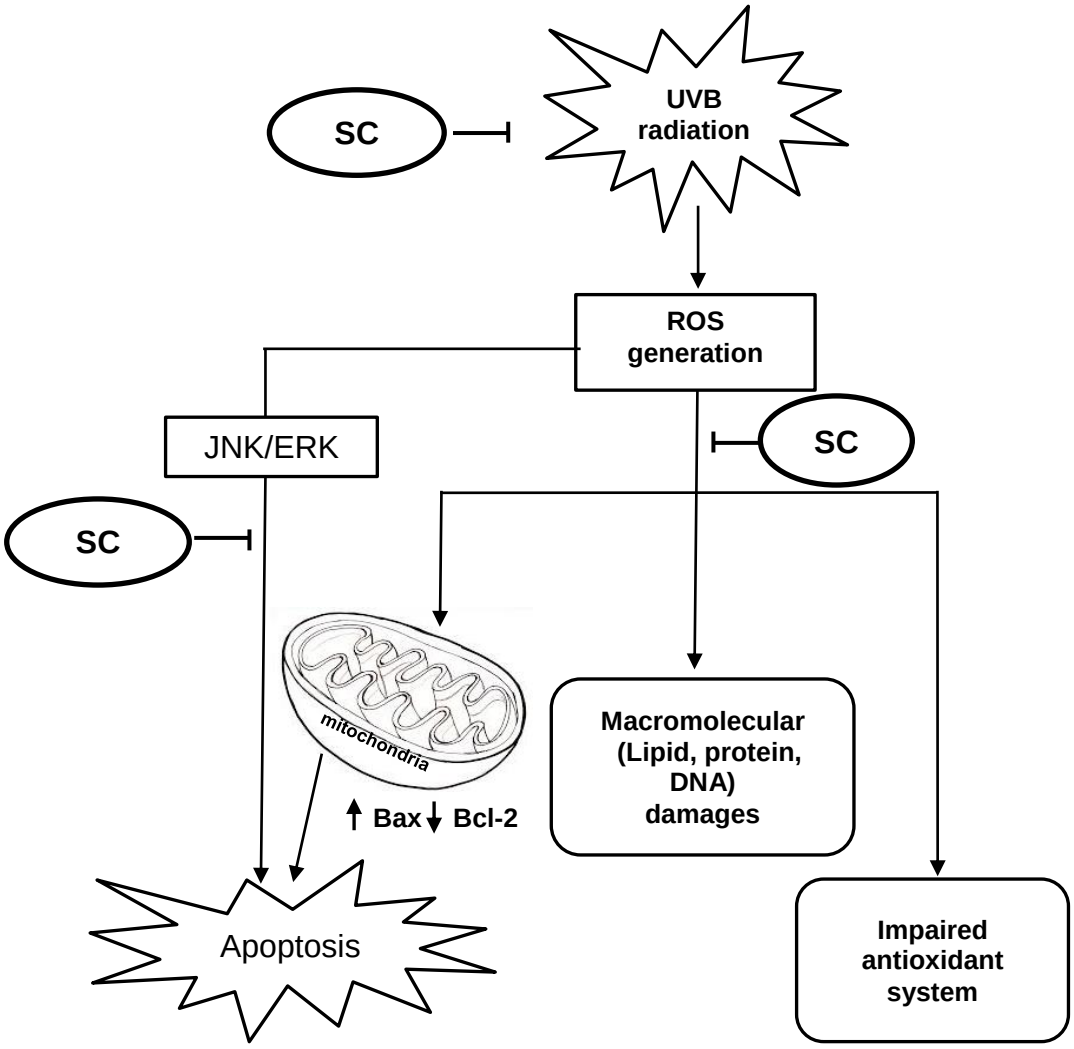


**Figure. 6.** Proposed pathway of SC-mediated cytoprotection against UVB-induced cell damage.

**The thesis for Degree of Master of Science in Medicine referring to experimental data and contents are from *Photo-protective effect of sargachromenol against UVB radiation-induced damage through modulating cellular antioxidant systems and apoptosis in human keratinocytes* which was published in the journal of *"Environmental Toxicology and Pharmacology"* with the"DOI: 10.1016/j.etap.2016.02.012.**

## 5. References


**1.** Ambothi, K., Nagarajan, R.P., 2014. Ferulic acid prevents ultraviolet B radiation induced oxidative DNA damage in human dermal fibroblasts. Int. J. Nutr. Pharmacol. Neurol. Dis. 4, 203-213.

**2.** Aoki, R., Aoki-Yoshida, A., Suzuki, C., Takayama, Y., 2014. Protective effect of indole-3-pyruvate against ultraviolet B-induced damage to cultured HaCaT keratinocytes and the skin of hairless mice. PloS One 9, e96804.

**3.** Beauchamp, M.C., Letendre, E., Renier, G., 2002. Macrophage lipoprotein lipase expression is increased in patients with heterozygous familial hypercholesterolemia. J. Lipid Res. 43, 215-222.

**4.** Carmichael, J., DeGraff, W.G., Gazdar, A.F., Minna, J.D., Mitchell, J.B., 1987. Evaluation of a tetrazolium-based semiautomated colorimetric assay: assessment of chemosensitivity testing. Cancer Res. 47, 936-942.

**5.** Choi, Y.J., Uehara, Y., Park, J.Y., Kim, S.J., Kim, S.R., Lee, H.W., Moon, H.R., Chung, H.Y., 2014. MHY884, a newly synthesized tyrosinase inhibitor, suppresses UVB-induced activation of NF-κB signaling pathway through the downregulation of oxidative stress. Bioorg. Med. Chem. Lett. 24, 1344-1348.

**6.** Dalle-Donne, I., Rossi, R., Giustarini, D., Milzani, A., Colombo, R., 2003. Protein carbonyl groups as biomarkers of oxidative stress. Clin. Chim. Acta 329, 23-38.

**7.** Dhanasekaran, D.N., Reddy, E.P., 2008. JNK signaling in apoptosis. Oncogene 27, 6245-

6251.

**8.** Heck, D.E., Gerecke, D.R., Vetrano, A.M., Laskin, J.D., 2004. Solar ultraviolet radiation as a trigger of cell signal transduction. Toxicol. Appl. Pharmacol. 195, 288-297.

**9.** Hewage, S.R.K.M., Piao, M.J., Kim, K.C., Cha, J.W., Xia, H., Choi, Y.H., Chae, S., Hyun, J.W., 2015. Galangin (3,5,7-Trihydroxyflavone) shields human keratinocytes from ultraviolet B-induced oxidative stress. Biomol. Ther. 23, 165-173.

**10.** Hur, S., Lee, H., Kim, Y., Lee, B.H., Shin, J., Kim, T.Y., 2008. Sargaquinoic acid and sargachromenol, extracts of Sargassum sagamianum, induce apoptosis in HaCaT cells and mice skin: Its potentiation of UVB-induced apoptosis. Eur. J. Pharmacol. 582, 1-11.

**11.** Kim, S., Lee, M.S., Lee, B., Gwon, W.G., Joung, E.J., Yoon, N.Y., Kim, H.R., 2014. Anti-inflammatory effects of sargachromenol-rich ethanolic extract of Myagropsis myagroides on lipopolysaccharide-stimulated BV-2 cells. BMC Complement. Altern. Med. 14, 231.

**12.** Kohno, M., Mizuta, Y., Kusai, M., Masumizu, T., Makino, K., 1994. Measurements of superoxide anion radical and superoxide anion scavenging activity by electron spin resonance spectroscopy coupled with DMPO spin trapping. Bull. Chem. Soc. Jpn. 67, 1085-1090.

**13.** Lee, K.O., Kim, S.N., Kim, Y.C., 2014. Anti-wrinkle effects of water extracts of teas in hairless mouse. Toxicol. Res. 30, 283-289.

**14.** Lee, S.J., Park, J.W., 2014. Enhancement of UVB radiation-mediated apoptosis by knockdown of cytosolic $NADP^+$-dependent isocitrate dehydrogenase in HaCaT cells.

BMB Rep. 47, 209-214.

**15.** Li, L., Abe, Y., Kanagawa, K., Usui, N., Imai, K., Mashino, T., Mochizuki, M., Miyata, N., 2004. Distinguishing the 5,5-dimethyl-1-pyrroline N-oxide (DMPO)-OH radical quenching effect from the hydroxyl radical scavenging effect in the ESR spin-trapping method. Anal. Chim. Acta. 512, 121-124.

**16.** Martinez, R.M., Pinho-Ribeiro, F.A., Steffen, V.S., Caviglione, C.V., Vignoli, J.A., Baracat, M.M., Georgetti, S.R., Casagrande, R., 2015. Hesperidin methyl chalcone inhibits oxidative stress and inflammation in a mouse model of ultraviolet B irradiation-induced skin damage. J. Photochem. Photobiol. B. 148, 145-153.

**17.** Rosenkranz, A.R., Schmaldienst, S., Stuhlmeier, K.M., Chen, W., Knapp, W., Zlabinger, G.J., 1992. A microplate assay for the detection of oxidative products using 2',7'-dichlorofluorescin-diacetate. J. Immunol. Methods 156, 39-45.

**18.** Saw, C.L., Yang, A.Y., Huang, M.T., Liu, Y., Lee, J.H., Khor, T.O., Su, Z.Y., Shu, L., Lu, Y., Conney, A.H., Kong, A.N.T., 2014. Nrf2 null enhances UVB-induced skin inflammation and extracellular matrix damages. Cell Biosci. 4, 39.

**19.** Singh, N.P. 2000. Microgels for estimation of DNA strand breaks, DNA protein crosslinks and apoptosis. Mutat. Res. 455, 111-127.

**20.** Yang, E.J., Ham, Y.M., Yang, K.W., Lee, N.H., Hyun, C.G., 2013. Sargachromenol from *Sargassum micracanthum* inhibits the lipopolysaccharide-induced production of inflammatory mediators in RAW 264.7 macrophages. Scientific World Journal 2013, 712303.

**21.** Yogianti, F., Kunisada, M., Ono, R., Sakumi, K., Nakabeppu, Y., Nishigori, C., 2012. Skin tumours induced by narrowband UVB have higher frequency of p53 mutations than tumours induced by broadband UVB independent of Ogg1 genotype. Mutagenesis 27, 637-643.

**22.** Zheng, J., Piao, M.J., Kim, K.C., Yao, C.W., Cha, J.W., Hyun, J.W., 2014. Fucoxanthin enhances the level of reduced glutathione via the Nrf2-mediated pathway in human keratinocytes. Mar. Drugs 12, 4214-4230.

## 6. Abstract in Korean

이번 연구에서는 human keratinocytes 에서 UVB로 인한 산화적 스트레스에 반대하는 사가 크로메놀의 항산화의 반영과 분자적인 기전을 통한 광화학적 예방 효과를 증명합니다. 사가크로메놀은 UVB로 인한 세포내 ROS 의 효과적인 소거능을 보여주었고, UVB로 인한 산화적인 고분자의 손상, protein carbonyl, DNA 손상과 지질과산화를 낮춰주었고, proapoptotic Bax, cleaved caspase 3 와 cleaved caspase 9 의 레벨을 낮춰주었으며 antiapoptotic protein 인 Bcl-2의 레벨을 올려주었습니다. 게다가 사가크로메놀은 UVB로 인해 감소된 superoxide dismutase, catalase, heme oxyganase-1 그리고 Nrf2 의 레벨 을 올려주었고, UVB로 인해서 증가된 JNK 와 ERK 의 레벨을 낮춰 주었습니다. 이번 실험결과에서는 사가크로메놀이 ROS로 인한 피부질환 의 약제개발의 가능성을 보여 주고, 세포의 항산화시스템에 영향을 주는 UVB 조사의 부정적 효과에 반대하여 세포보호 를 할수 있음을 보여 줍니다.

## 7. Acknowladgements

I am very much pleased having the opportunity to study under the supervision of Prof. Jin Won Hyun. First and foremost I would like to express my deepest and sincere gratitude to my supervisor in charge Prof. Jin Won Hyun, for providing me this valuable opportunity to commence my master degree In Jeju National University and for keen attention throughout my study, valuable suggestions and critical reviews of the reports rendered to me during my studies which made the foundation for success of my two years study in Republic of Korea.

I am also grateful to Prof. Park Deok Bae and Prof. Kang Hee Kyoung, School of medicine Jeju National University, who provided valuable instructions and suggestions to complete my thesis. Further all the professors guided me in the school of Medicine are sincerely appreciated.

I am honored to place my heartfelt gratitude towards Dr. Mei Jing Piao who gave me a relentless support, regardless of the time as well as language barriers. Also, my former seniors and colleges Ji Won Cha, Susara Maddumahewage and Han Xia were always behind my progress. My lab was my home as my colleague cared me a lot within these two years. Dear Min Chang Oh, Park jeong eon, Moon You Jin and Yoon Hae Kyung, I am too much lucky to being a part of your company.

My special thanks goes to Prasad Tharanga Jayasooriya, Dilshara Matharage for guiding, supporting and encouraging me reach my goals. I am grateful to my classmate, friend and roommate Susara madduma hewage for strengthening and supporting me at every hard time. During the period of two years, many friends were helpful to color my life. I use this opportunity to acknowledge all my colleagues in Jeju National University for making those joyful memories.

Further I owe my gratitude to my former supervisors Dr. Barana Jayawardana, Dr. Janak Vidanarachchi, and Thusith Samarakoon Faculty of Agriculture, University of Peradeniya,

Sri Lanka who directed me for higher studies.

Finally, I want to thank my beloved parents and my family members who were waiting to see my success and encouraged my works all my life.